

Valley polarized electronic beam splitting in graphene

J.L. Garcia-Pomar¹, A. Cortijo¹, and M. Nieto-Vesperinas¹

¹*Instituto de Ciencia de Materiales de Madrid, Consejo Superior de Investigaciones Científicas, Campus de Cantoblanco, Madrid 28049, Spain.**

We show how the trigonal warping effect in doped graphene can be used to produce fully valley polarized currents. We propose a device that acts both as a beam splitter and a collimator of these electronic currents. The result is demonstrated through an optical analogy using two dimensional photonic crystals.

PACS numbers: 73.23.Ad, 85.75.-d, 42.70.Qs, 42.79.Fm, 81.05.Uw, 73.63.-b

Since its recent synthesis [1] graphene is proving to be a fruitful system in which ideas coming from varied areas of physics successfully merge: soft condensed matter [2], *pseudorelativistic* quantum electrodynamics [3] and, more recently, optics [4] and *valleytronics* [5]. The concept of *valleytronics* [5] describes the use of the valley degeneracy in graphene as a degree of freedom to carrying information in the same way as the spin does in spintronic. In the scheme proposed in [5] the generation and detection of the valley polarized current are achieved by means of a quantum point contact in a graphene ribbon. The main difficulty in the experimental realization of this approach comes from the necessity of tailoring the graphene samples into nanoribbons and quantum point contacts with zigzag edges needed to support edge states. In this letter we propose an alternative mechanism for getting a different response from each valley using the effect of the trigonal warping [6] that can be tuned by a gate voltage in graphene samples of arbitrary shapes. The main idea relies on the fact that at energies where the trigonal warping is noticeable, the Fermi surfaces around each valley are different and anisotropic. This allows us to suggest a device based on a p-n junction where the response is valley asymmetric. (Figs. 1 and 2).

In the tight-binding approximation of the low energy band structure for graphene, the dispersion relation including both the Dirac and the TW terms, is:

$$E_s(\mathbf{k}) = \pm \hbar v_F \sqrt{k^2 + \frac{a^2}{16} k^4 + \frac{a}{2} s (k_x^3 - 3k_x k_y^2)}, \quad (1)$$

where v_F is the Fermi velocity, a is the lattice constant and the short notation $k^2 = k_x^2 + k_y^2$ is used. The parameter $s = \pm 1$ refers to the two valleys.

The average current moving through the sample is $\langle \mathbf{J}_s \rangle = \frac{e}{\hbar} |t_s|^2 \mathbf{v}_{g,s}$, where t_s represents the transmission coefficient and $\mathbf{v}_{g,s}$ stands for the group velocity in each valley. When the TW term is considered, $\mathbf{v}_{g,s}$ has the form

$$\mathbf{v}_{g,s} = \frac{1}{\hbar} \nabla_{\mathbf{k}} E_s(\mathbf{k}) = \pm \frac{v_F^2}{2E_s(\mathbf{k})} \left(\left(2 + \frac{a^2}{4} k^2\right) \mathbf{k} + \frac{a}{2} s \mathbf{F} \right), \quad (2)$$

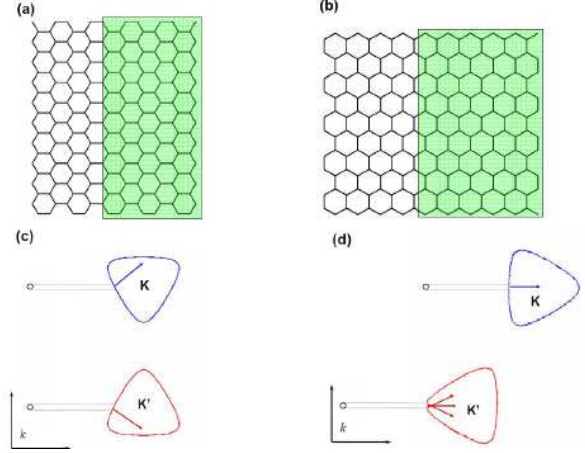


FIG. 1: (Color online) The two limiting cases for the deposition of the gate over the graphene sample. The green area denotes the region doped with holes at energies where the TW becomes relevant. (a) Interface of the gate parallel to the zigzag orientation and (b) the armchair interface. (c) and (d) represent the corresponding isofrequency lines showing the conservation of the parallel wavevector for the zigzag and armchair interface, respectively. We obtain two directions of refraction for the zigzag orientation parallel to the interface depending on whether the chosen valley is K or K' . For the armchair interface, a forward direction of refraction appears due to the little dispersion produced by the second valley.

where $\mathbf{F} = (3k_x^2 - 3k_y^2, -6k_x k_y)$. When TW is considered, $|t_s|^2$ does not essentially differ from that obtained when only the linear term is considered in the whole $p - n$ junction [3, 7] having almost the same shape for both valleys. The major role in the different behavior of $\langle \mathbf{J}_s \rangle$ for each valley is played by the group velocity $\mathbf{v}_{g,s}$, since it explicitly depends on s .

It is well known that optical and electronic systems share many wave-like properties. A $p - n$ junction in graphene has an photonic analogy with an optical system composed of two effective media with opposite signs of their refractive index. In optical material slabs with negative refractive index, Snell's law leads to the phenomenon of light focussing [8, 9]. A similar behavior has been proposed in graphene for electrons [4]. If the

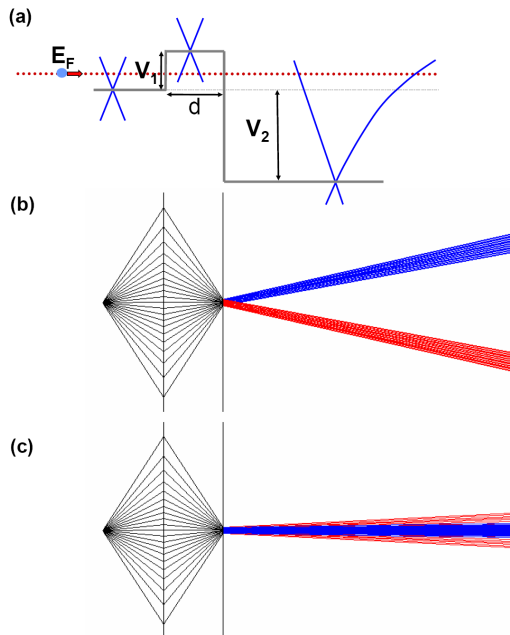


FIG. 2: (Color online) (a) Potential profile of a $n-p-n$ junction and schematic band structure of one valley. (b) Theoretical ray tracing of the beams coming from a point source in a junction with the interface parallel to the zigzag orientation. $E_F = 0.05eV$, $V_1 = 0.10eV$ and $V_2 = -1.5eV$. The beam splitting is noticeable. (c) Armchair junction. We now obtain a collimation perpendicular to the interface.

Fermi level is chosen such that the conduction band, (for which the group velocity \mathbf{v}_g points *outwards* the energy surface), in one side of the junction, is connected to the valence band in the other side, (where \mathbf{v}_g now points *inwards* the energy surface), the system behaves as the electrical counterpart of a Veselago Lens [8].

In Fig.1 we show a field effect $n-p^+$ device in graphene. In the p^+ area, the applied gate voltage is such that the chemical potential is located at energies where the TW effect becomes relevant (according to ARPES data [10] this appens for energies of $0.6 - 0.7eV$). When the TW term is considered, the band is no longer isotropic around each K point. We have then to care about the relative orientation between the lattice and the deposited gate. Due to the symmetry of the honeycomb lattice, all the possible orientations lie between the two limiting cases shown in Figs.1(a),(b). Fig.1(c) shows the direction of $\mathbf{v}_{g,s}$ determined by conservation of the momentum parallel to the potential barrier interfaces when the boundary is parallel to the zigzag orientation. Due to the s dependence of $\mathbf{v}_{g,s}$ the currents associated to each valley travel in different directions leading to two different currents polarized in the valley index. Fig.1(d) represents the parallel momentum conservation when the gate is oriented along the armchair direction. The current associated to one of the valleys (valley K) is fully collimated because,

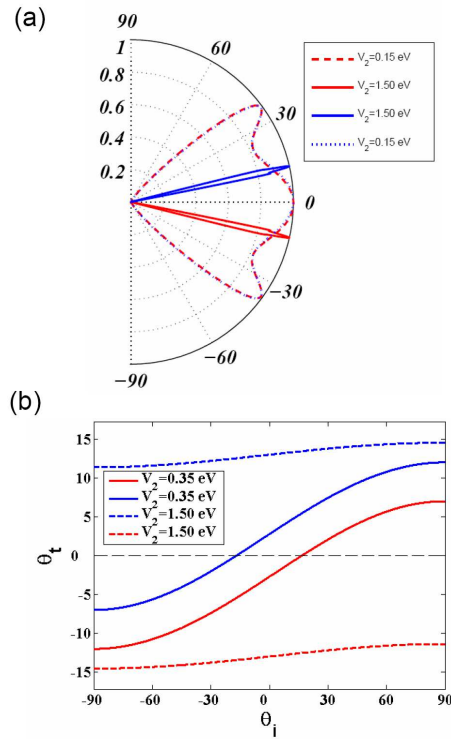


FIG. 3: (Color online) (a) Transmission probability for the K (blue lines) and K' (red lines) as a function of the output angle θ_t for different negative potentials V_2 . The parameters are: barrier width: $d = 100nm$, initial energy: $E_F = 0.05eV$, initial potential: $V_1 = 0.14eV$. (b) Output angle θ_t of the electronic beam as a function of the incident angle θ_i for valleys K (upper blue lines) and K' (lower red lines). (See text). Barrier width: $100nm$, initial energy $E_F = 0.05eV$, first potential step: $V_1 = 0.10eV$.

by momentum conservation, the accessible area of the energy surface is almost plane. The current belonging to the other valley is more dispersed because the accessible area has a higher curvature. With these characteristics, we can design a device to achieve the realization of a beam splitter with an $n-p-n$ junction (Fig. 2(a)) with the interface parallel to the zigzag orientation. In the first zone, we introduce an electron source. In this region, the Fermi level E_F is at low energy in the conduction band, where the Fermi surface is circular and the linear Dirac regime is valid. This area is separated from a zone of low chemical potential (p -region) in the valence band, by a barrier with a potential V_1 . In the interface we have both negative refraction and focusing [4]. The last step with negative potential V_2 is placed immediately before the electron focusing in order to get a very small illuminated zone. In this way, we have narrower exit beams avoiding the formation of caustics which would appear if the position of the focus were reached before the last interface. Finally, the last region is at high

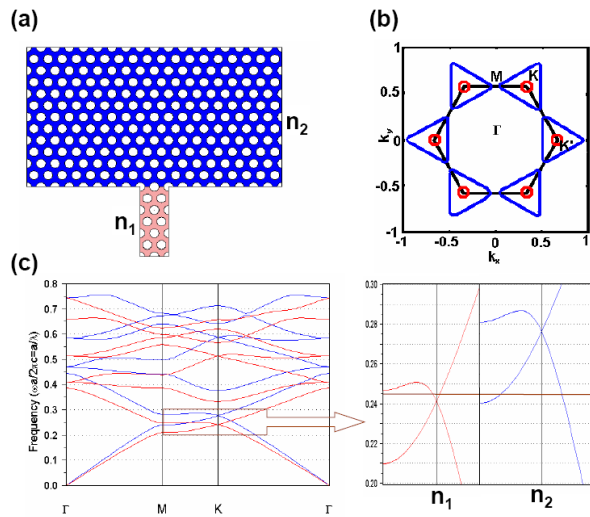


FIG. 4: (Color online) (a) Geometry of the trigonal photonic crystal (PC) of air holes and optical analogy of a p-n junction in graphene. (b) Brillouin zone and isofrequency lines for the two PCs for n_1 (red circles) and for n_2 (blue triangles). (c) Band diagram for a trigonal photonic crystal of air holes with radius $r = 0.33a_{PC}$ in a dielectric matrix with refractive index $n_1 = 3.04$ (red bands) and $n_2 = 2.65$ (blue bands). The two insets show details of the zone around the K point where we observe that for the wavelength $\lambda = 4.08a_{PC}$, n_1 corresponds to the conduction band, whereas n_2 is located at the TW valence band.

voltages in the conduction band (n^- -region) i.e. it has a strong TW. A polarization of valley occurs, this giving rise to a beam splitting of the electronic beams belonging to different valleys (Fig.2(b),(c)). Fig.3 shows the two beams obtained for a potential $V_2 = -1.5eV$ (TW case) 25.4° apart from each other for maximum of transmission. The beam dispersion is approximately only 3° . In the Dirac regime (lower energies) we observe that the splitting of the beams is reduced.

A different situation occurs if the interface is parallel to the armchair orientation. In this configuration, (Fig. 1(b)) the beam of one valley is strongly collimated and waveguided (blue color in Fig.2(b)) due to the flat portion of the isofrequency line. The other valley slightly disperses the beam. Due to the big difference of curvatures between the Dirac and the TW isoenergies, the allowed wavevectors \mathbf{k} are situated in a zone of the TW isoline with small curvature involving a low dispersion (red color in Fig.2(b)).

Up to day, the most efficient way of identifying graphene samples is by optical contrast [11]. The maximum of this contrast depends both on the thickness of the substrate and on the wavelength of the monochromatic radiation used to illuminate the sample, usually in the visible range. For this range, the maximum contrast corresponds to a thickness of $300nm$ and the values reached

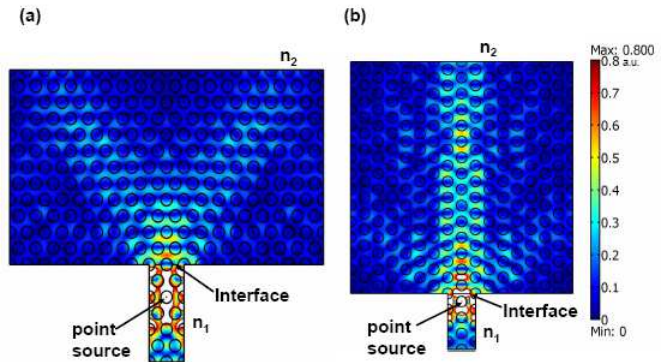


FIG. 5: (Color online) Maps of the electric field modulus of a wave originated at a point source located inside a photonic crystal with refractive index n_1 and propagating through another photonic crystal of dielectric matrix n_2 . (a) Armchair orientation, illustrating the beam splitting of the two different valleys K and K' . (b) Zigzag orientation. We can see a collimation of the beams since the curvature in the trigonal distorted band is smaller than the one of the circular isoline in the proximity of the Dirac point. The angular dispersion is low.

for the chemical potential are of the order of $0.3eV$. However, it is theoretically found [12] that another maximum in the contrast appears at a thickness of $90 - 100nm$. With this range, it is possible to get values of the chemical potential up to $0.6eV$, just in the threshold where the TW starts to be appreciable. The effect discussed here can then be effectively observed with minor experimental changes in current samples, like increasing the gate voltage and decreasing the substrate thickness.

An optical analogy. Control of beam propagation, collimation and focusing in photonic crystals (PCs) is already well developed [13, 14, 15, 16, 17], thus one can assess the validity of the above analysis for graphene by putting forward its analogy with this photonic system. In fact, an optical analogy of the graphene system was previously described [18, 19]. We can realize it with a 2-D PC with honeycomb, kagome or trigonal structure where the gap between the first and second bands is replaced by a Dirac point in the K point of symmetry. As an example, we have used a trigonal lattice, with parameter a_{PC} , of air cylinders of radius $r = 0.33a_{PC}$ inside a dielectric matrix with refractive index n (Fig.4(a)). We notice that, in the case of the trigonal lattice, the Brillouin zone (BZ) (Fig.4(b)) coincides with the real lattice, while in the graphene honeycomb lattice the BZ is rotated 30 degrees with respect to the real lattice, which implies that the zigzag and armchair situations described in graphene are exchanged in the PC. Now we cannot change the light frequency throughout the crystal like we change the chemical potential in a transistor of field effect in graphene, but we can displace the frequency position

of the Dirac point in the band diagram by slightly varying the refractive index of the dielectric matrix (Fig.4(c)). In this way, a junction of two PCs with the same trigonal structure but with slightly different refractive index, mimics the field effect transistor in graphene.

Fig.5 shows a finite elements numerical simulation of the electric field modulus distribution from a point source, emitting TE polarized light (i.e. the electric field is parallel to the long axis of the air holes) with a wavelength $\lambda = 4.08a_{PC}$ in a dielectric matrix with refractive index $n_1 = 3.04$ together with another PC of the same structure but a slightly smaller refractive index $n_2 = 2.65$ for the two limiting cases: armchair(Fig.5(a)) and zigzag (Fig.5(b)). The creation of a beam splitter in the latter PC for the armchair situation is illustrated by the fact that the two isofrequency curves in the K and K' points are triangles pointing in opposite directions from each other (right and left). Conversely, if we put the zigzag structure parallel to the interface, we obtain a collimation of the beams.

To summarize, we have proposed an efficient way to get *valley polarized* beams using the trigonal warping effect in the graphene bands. We have shown a possible design of a beam splitter and a collimator device. This formation of valley polarized beams, is a key ingredient for the use of this new polarization in graphene as an effective information carrying degree of freedom. Besides, the transport properties of graphene can constitute a useful and novel device in future nanoelectronics. Finally, we have checked the validity of these phenomena, by means of an optical analogy with two dimensional photonic crystals and proposed a theory of isofrequency lines as a useful tool to simulate these kind of processes in graphene systems.

Acknowledgements

We gratefully acknowledge illuminating discussions and useful comments of Prof. María A. H. Vozmediano and Ramon Aguado. Work supported by the Spanish DGICYT and the European Union. J.L. G.-P. acknowledges I3P grant program. A. C. acknowledges MEC of Spain for financial support.

-
- * Electronic address: jlgarcia@icmm.cisc.es; Electronic address: cortijo@icmm.csic.es; Electronic address: mnieto@icmm.csic.es
- [1] K. S. Novoselov, A. K. Geim, S. V. Morozov, D. Jiang, M. I. Katsnelson, I. V. Grigorieva, S. V. Dubonos, and A. A. Firsov, *Nature* **438**, 197 (2005).
 - [2] A. Fasolino, J. H. Los, and M. I. Katsnelson, [arXiv.org:cond-mat/0704.1793](https://arxiv.org/abs/cond-mat/0704.1793) (2007).
 - [3] M. I. Katsnelson, K. S. Novoselov, , and A. K. Geim, *Nature Physics* **2**, 620 (2006).
 - [4] V. V. Cheianov, V. Fal'ko, and B. L. Altshuler, *Science* **315**, 1252 (2006).
 - [5] A. Rycerz, J. Tworzydło, and C. W. J. Beenakker, *Nature Physics* **3**, 172 (2007).
 - [6] R. Saito, G. Dresselhaus, and M. S. Dresselhaus, *Phys. Rev. B* **61**, 2981 (2000).
 - [7] V. V. Cheianov and V. I. Falk'o, *Phys. Rev. B* **74**, 041403(R) (2006).
 - [8] V. G. Veselago, *Sov. Phys. Usp.* **10**, 509 (1968).
 - [9] J. B. Pendry, *Phys. Rev. Lett.* **85**, 3966 (2000).
 - [10] S. Y. Zhou, G.-H. Gweon, J. Graf, A. V. Fedorov, C. D. Spataru, R. D. Diehl, Y. Kopelevich, D.-H. Lee, S. G. Louie, and A. Lanzara, *Nature Physics* **2**, 595 (2006).
 - [11] K. S. Novoselov, A. K. Geim, S. V. Morozov, D. Jiang, Y. Zhang, S. V. Dubonos, I. V. Grigorieva, and A. A. Fisov, *Science* **306**, 666 (2004).
 - [12] P. Blake, K. S. Novoselov, A. H. C. Neto, D. Jiang, R. Yang, T. J. Booth, A. K. Geim, and E. W. Hill, *Appl. Phys. Lett.* **91**, 063124 (2007).
 - [13] H. Kosaka, T. Kawashima, A. Tomita, M. Notomi, T. Tamamura, T. Sato, and S. Kawakami, *Appl. Phys. Lett.* **74**, 1212 (1999).
 - [14] M. Notomi, *Phys. Rev. B* **62**, 10696 (2000).
 - [15] X. Wang, Z. Ren, and K. Kempa, *Opt. Express* **12**, 2919 (2004).
 - [16] J. L. Garcia-Pomar and M. Nieto-Vesperinas, *Opt. Express* **13**, 7997 (2005).
 - [17] P. T. Rakich, M. S. Dahlem, S. Tandon, M. Ibanescu, M. Soljac, G. S. Petrich, J. D. Joannopoulos, L. A. Kolodziejski, and E. P. Ippen, *Nature Materials* **5**, 93 (2006).
 - [18] F. Haldane and S. Raghu, [arXiv.org:cond-mat/0503588](https://arxiv.org/abs/cond-mat/0503588) (2005).
 - [19] R. A. Sepkhanov, Y. B. Bazaliy, and C. W. J. Beenakker, *Phys. Rev. A* **75**, 063813 (2007).